© AUG 2026 | IRE Journals | Volume 10 Issue 2 | ISSN: 2456-8880
DOI: https://doi.org/10.64388/IREV10I2-1722428

Adaptive Boundary Control of an Euler–Bernoulli Overhead Bridge under Moving Vehicle Loads with Uncertain Boundary Stiffness: Explicit Incorporation of Disturbance Effects in the Lyapunov Stability Analysis.

CHUKWUEMEKA PAUL AMADI[1], EMMANUEL IGEY[2]
[1,2]Department of Mathematics, Faculty of Sciences Rivers State University, Port Harcourt, Nigeria.
ORCID: 0000-0003-2896-2087[1], 0009-0001-9119-0983[2]

Abstract- This study examines the adaptive boundary control of an Euler–Bernoulli overhead bridge subjected to moving vehicle loads under uncertain boundary stiffness, with particular attention to the influence of external disturbances on Lyapunov stability. A Galerkin reduced-order model based on the fundamental mode is used to describe the bridge dynamics, while an adaptive boundary-control strategy is developed to compensate for boundary-stiffness uncertainty and reduce vibration caused by the moving vehicle. The vehicle load is incorporated explicitly as a time-dependent bounded disturbance, and a disturbance-inclusive Lyapunov approach is employed to establish the uniform ultimate boundedness (UUB) of the closed-loop system. Numerical results show that the vehicle reaches the 10 m bridge exit at approximately, producing the most significant transient response, after which the modal displacement, velocity, control effort, and Lyapunov measures decrease rapidly as the disturbance leaves the bridge. The corresponding spatial deflection profiles confirm the effective attenuation of the bridge response following vehicle departure, while the Lyapunov analysis indicates that the controlled states remain bounded and gradually approach the desired operating condition. Overall, the findings demonstrate that the proposed adaptive boundary-control strategy can effectively reduce transient vibrations and maintain stable bridge dynamics despite uncertain boundary stiffness, thereby providing numerical support for the disturbance-inclusive UUB stability framework.

Keywords: Euler–Bernoulli bridge; adaptive boundary control; moving vehicle load; uncertain boundary stiffness; Lyapunov stability; uniform ultimate boundedness; disturbance rejection; Galerkin method.

I. INTRODUCTION

Bridge structures are continually subjected to dynamic loads from moving vehicles, which can produce vibrations that influence structural performance. The magnitude of these vibrations depends on several factors, including vehicle speed and load, bridge stiffness and damping, boundary conditions, and the interaction between the moving vehicle and the bridge response. Excessive vibrations can reduce serviceability and driving comfort, accelerate structural deterioration, and, in severe cases, compromise safety. The Euler–Bernoulli beam model provides a suitable mathematical framework for describing the dominant bending behaviour of slender bridge structures. However, real bridge supports rarely have perfectly known or constant stiffness. Uncertainty may result from bearing flexibility, foundation settlement, environmental conditions, material deterioration, ageing, and construction-related variations. These uncertainties can significantly influence the dynamic response of the bridge and therefore need to be considered when developing an effective vibration-control strategy.

Bridge vibration induced by moving vehicles has received considerable attention because the interaction between traffic loads and structural dynamics can significantly influence bridge response. Pourzeynali et al. (2021) investigated moving-load identification for bridge structures using an explicit form of the Newmark-β method. Their study included numerical investigations of a simply supported bridge and a three-span continuous bridge, together with experimental validation using a sensor-equipped simply supported bridge. The authors examined the effects of sensor number and location, measurement noise, surface roughness, sampling frequency, and vehicle speed. Their results demonstrate the importance of accurate moving-load identification in bridge monitoring and dynamic assessment.

More detailed vehicle–bridge interaction models have subsequently been developed to capture the complex dynamic behaviour associated with moving vehicles. Dong et al. (2023) developed a vehicle–bridge interaction element and implemented it in ABAQUS using a user-defined element. Their formulation provides a computational framework for simulating coupled vehicle–bridge dynamics and was verified through numerical examples, including a high-speed railway bridge application. Similarly, Shi et al. (2024) developed an improved vehicle–bridge interaction model that accounted for contact-patch size and vehicle self-generated excitation. Their results showed that contact-patch characteristics can influence the appropriate simulation time step and the frequencies that can be identified from the response.

The theoretical foundations of moving-load and vehicle–bridge interaction analysis have also been extensively established. Ouyang (2011) provided a comprehensive treatment of moving-load dynamic problems, highlighting the distinctive characteristics of structures subjected to moving forces and masses. Yang and Lin (2005) Investigated vehicle–bridge interaction dynamics using modal superposition and demonstrated that the dynamic responses of both the bridge and vehicle are influenced by the interaction between vehicle excitation and structural natural frequencies. Their work also showed that, under appropriate conditions, the first bridge mode can provide a useful approximation of the dominant structural response. In another important contribution, Xia et al. (2000) investigated the dynamic interaction between long suspension bridges and running trains using a three-dimensional finite-element bridge model coupled with vehicle dynamics. Their study demonstrated the importance of considering wheel–track contact forces in coupled vehicle–bridge analyses.

Uncertainty in structural stiffness is another important consideration in bridge dynamics and structural health monitoring. You et al. (2023) developed an adaptive inverse unit-load method for distributed reconstruction of bridge bending stiffness using onboard deflection data. Their two-stage methodology first estimated the stiffness using uniform discretization and subsequently optimized the element-node distribution to improve the reconstructed stiffness field. Numerical and experimental investigations demonstrated the effectiveness of the method for estimating distributed bridge stiffness. Although this approach provides an effective means of estimating bridge stiffness, it is primarily concerned with stiffness identification rather than real-time vibration suppression through adaptive boundary control.

Adaptive boundary control has been developed extensively for distributed-parameter systems with uncertain parameters. Krstić and Smyshlyaev (2008) studied the adaptive boundary controllers for unstable parabolic partial differential equations containing unknown destabilizing parameters. Their work established adaptive boundary-control techniques without requiring relative-degree limitations, open-loop stability assumptions, or actuation throughout the spatial domain. This contribution provides an important theoretical foundation for adaptive control of distributed-parameter systems when system uncertainties cannot be directly measured.

Building on this framework, He et al, (2014) developed an adaptive boundary-control strategy for a class of inhomogeneous Timoshenko beam equations subject to boundary-output constraints. An integral-barrier Lyapunov function was employed to prevent constraint violation, while adaptive laws were introduced to compensate for system uncertainties. The proposed method achieved vibration suppression without requiring discretization or spatial simplification of the beam dynamics. Although this work is closely related to the present study from the perspective of adaptive boundary control, it considered Timoshenko beam dynamics rather than an Euler–Bernoulli bridge subjected to moving vehicle excitation.

Adaptive control has also been applied to moving distributed-parameter systems. Wang and Krstić (2021) developed an adaptive event-triggered boundary-control strategy for a load-moving cable system represented by a coupled hyperbolic PDE–ODE model. Their study considered uncertainties in the stiffness and damping of the viscoelastic guideway and developed an adaptive output-feedback boundary controller. The overall closed-loop system was analysed using Lyapunov methods, and numerical simulations demonstrated vibration suppression for a mining cable elevator. This study is particularly relevant to the present work because it demonstrates how adaptive boundary control can be combined with a moving-load system. Nevertheless, the physical system considered was a cable elevator rather than an overhead bridge, and the uncertainty structure differs from the uncertain boundary stiffness considered here.

For Euler–Bernoulli structures specifically, Abdelkarim and Saedpanah (2023) investigated stabilization of an axially moving Euler–Bernoulli beam using adaptive boundary control. They developed a low-gain adaptive velocity-feedback controller and established exponential stability of the closed-loop system using nonlinear semigroup theory. Numerical simulations were also provided to illustrate the theoretical results. While this study confirms the applicability of adaptive boundary control to Euler–Bernoulli systems, its focus was an axially moving beam rather than a stationary bridge subjected to an externally moving vehicle load.

More recently, Wang et al. (2025) investigated adaptive vibration control of an Euler–Bernoulli beam with an unknown payload. Their approach employed an adaptive boundary controller to compensate for the unknown payload parameter. The authors established well-posedness using a linear-operator semigroup framework and derived asymptotic stability of the closed-loop system using an extended Krasovskii–LaSalle invariance principle. This study is closely related to the present work because both consider adaptive boundary control of Euler–Bernoulli systems. However, the uncertainty in Wang et al, (2025) is associated with an unknown payload rather than uncertain boundary stiffness, and their model does not explicitly incorporate a moving vehicle load as an external disturbance.

Cui et al, (2025) proposed an event-triggered adaptive-control strategy for a rotating disk–beam–mass system with time-varying boundary constraints. Their method incorporated parametric uncertainty and used a tangent-type barrier Lyapunov function to ensure that time-varying constraints were satisfied while maintaining closed-loop stability. Although the study demonstrates the effectiveness of adaptive event-triggered boundary control for uncertain flexible structures, its application to a rotating disk–beam–mass system does not address the dynamic response of bridge structures under moving vehicle loads.

Sun et al, (2025) further developed an event-triggered adaptive safe-oriented boundary-control strategy for flexible beam systems described by uncertain Euler–Bernoulli PDEs. Their formulation considered uncertainties in damping and bending stiffness together with boundary disturbances and used a barrier-Lyapunov-based framework to establish safety and stability. This work represents an important recent development in adaptive boundary control of uncertain Euler–Bernoulli systems. However, it does not explicitly address the combined effects of moving vehicle excitation and uncertain boundary stiffness in an overhead bridge.

Adaptive structural mechanisms have also been investigated from a broader structural-engineering perspective. Gambarelli et al, (2023) examined an adaptive concrete beam with integrated fluidic actuators using nonlinear three-dimensional finite-element analysis. Their results demonstrated the potential of adaptive mechanisms to influence structural deformation and failure behaviour. Such studies emphasize the growing role of adaptive structural systems, although they focus primarily on structural adaptation rather than Lyapunov-based adaptive boundary control.

The existing literature demonstrates substantial progress in four interconnected areas: moving-load and vehicle–bridge interaction modelling, bridge stiffness estimation, adaptive boundary control of

© AUG 2026 | IRE Journals | Volume 10 Issue 2 | ISSN: 2456-8880
DOI: https://doi.org/10.64388/IREV10I2-1722428

distributed-parameter systems, and adaptive vibration control of Euler–Bernoulli structures. However, these areas have largely been examined separately, leaving limited research that integrates them into a unified framework for bridge vibration control under realistic operating uncertainties.

Studies on moving loads have primarily focused on vehicle–bridge interaction and moving-load identification, with emphasis on factors such as vehicle speed, load characteristics, sensor configuration, and structural response (Pourzeynali et al., 2021; Dong et al., 2023; Shi et al., 2024). Similarly, research on bridge stiffness has concentrated mainly on identifying, estimating, or reconstructing stiffness distributions from structural response measurements (You et al., 2023). In contrast, adaptive boundary-control studies have predominantly addressed beams, cables, and other distributed-parameter systems with uncertain system parameters, demonstrating the effectiveness of adaptive control and Lyapunov-based stability techniques (Krstić & Smyshlyaev, 2008; He et al., 2014; Wang & Krstić, 2021; Abdelkarim & Saedpanah, 2023; Wang et al., 2025; Sun et al., 2025). The present study addresses this gap by employing a Galerkin reduced-order model to represent the bridge dynamics and developing an adaptive boundary controller capable of estimating and compensating for the uncertain boundary stiffness online. In addition, the moving vehicle load is explicitly retained in the reduced-order model and treated as a bounded disturbance rather than being neglected or absorbed into the nominal system dynamics. Its contribution is then incorporated directly into the Lyapunov stability analysis, allowing the effects of the external disturbance to be quantified in the closed-loop stability condition. This formulation provides a rigorous basis for establishing the uniform ultimate boundedness (UUB) of the controlled bridge response and for determining an explicit ultimate bound under moving-vehicle excitation and boundary-stiffness uncertainty.

II. MATHEMATICAL FORMULATION

Let's consider an Euler–Bernoulli bridge of length L. Let w(x,t) denote its transverse displacement.

$$\rho A\frac{\partial^2 w}{\partial t^2}+c\frac{\partial w}{\partial t}+EI\frac{\partial^3 w}{\partial x^3}=f(x,t) \tag{1}$$

ρA is the mass per unit length, c is the damping coefficient, EI is the flexural rigidity, and $f(x,t)$ is the moving-vehicle load.

$$f(x,t)=\sum P_i\delta[x-x_i(t)] \tag{2}$$

P_i is the magnitude of the ith vehicle load, $x_i(t)$ is its position, and δ is the Dirac delta function.

$$x_i(t)=x_i(0)+v_it \tag{3}$$

We employ the Galerkin Reduced-Order Model, we have;

$$y(x,t)=\sum \varphi_r(x)q_r(t) \tag{4}$$

Assuming that the bridge response is dominated by its fundamental mode, the transverse displacement is approximated by

$$y(x,t)=\varphi(x)q(t)$$

where is the fundamental mode shape and is the associated modal coordinate.

$$m\frac{\partial^2 q}{\partial t^2}+c_m\frac{\partial q}{\partial t}+k_mq=d_m(t) \tag{5}$$

$$d(t)=\left(\frac{1}{m}\right)\sum P_i\varphi[x_i(t)] \tag{6}$$

For the adaptive boundary controller, we have;

$$m\frac{\partial^2 q}{\partial t^2}+c_m\frac{\partial q}{\partial t}+k_mq=u+d_m(t) \tag{7}$$

$$u=-k_pq-k_v\frac{\partial q}{\partial t}-\hat{k}q \tag{8}$$

$$\tilde{k}=k-\hat{k} \tag{9}$$

The adaptive law is given by;

$$\hat{k} = -\Gamma q \frac{\partial q}{\partial t}$$

Hence: $\tilde{k} = \Gamma q \frac{\partial q}{\partial t}$

We consider the state-space model

$$\frac{\partial q}{\partial t} = x_2 \quad (10)$$

$$\dot{x}_2 = -c_c x_2 - k_p x_1 - \tilde{k} x_1 + d(t) \quad (11)$$

$$X = [q, \dot{q}, \tilde{k}]^T$$

We obtain the Lyapunov Stability Analysis by;

$$V = \frac{1}{2}\dot{q}^2 + \frac{1}{2}k_p q^2 + \left(\frac{1}{2\Gamma}\right)\dot{k}^2 \quad (12)$$

For $k = 20, k_p = 25, \Gamma = 15$

Equation (12) becomes

$$V = \frac{1}{2}\dot{q}^2 + 22.5q^2 + \left(\frac{1}{30}\right)\dot{k}^2$$

Thus V is positive definite and satisfies $c_1||X||^2 \leq V \leq c_2||X||^2$, $c_1||X||^2 \leq V \leq c_2||X||^2$, with $c_1 = \frac{1}{30}$

Now we find the disturbance and Lyapunov derivative such that;

$$\dot{V} = -c_c\dot{q}^2 + \dot{q}d(t) \quad (13)$$

Assume $|d(t)| \leq d_{max}$

$$\dot{V} \leq -c_c\dot{q}^2 + d_{max}|\dot{q}| \quad (14)$$

Using young's inequality: $\dot{V} \leq -\left(c_c - \frac{\varepsilon}{2}\right)\dot{q}^2 + \frac{{d_{max}}^2}{(2\varepsilon)}$

$c_c = 10.8$ and $\varepsilon = 20.8$: $\dot{V} \leq -5.4\dot{q}^2 + \frac{{d_{max}}^2}{21.6}$

For strict Lyapunov and UUB

$$V_s = V + \eta q\dot{q} \quad (15)$$

For sufficiently small $\eta > 0$, $cc_1||X||^2 \leq V_s \leq c_2||X||^2$ After bounding the cross and disturbance terms, choose the design constants so that:

$$\dot{V}_s \leq -\alpha V_s + \beta \quad (16)$$

where $\alpha > 0$ and $\beta \geq 0$

$$V_s(t) \leq V_s(0)e^{-\alpha t} + \left(\frac{\beta}{\alpha}\right)(1 - e^{-\alpha t}) \quad (17)$$

$$\lim_{t\to\infty} \sup||X(t)|| \leq \frac{\beta}{\alpha} \quad (18)$$

Therefore, the closed-loop system is uniformly ultimately bounded with;

$$R = \sqrt{\frac{\beta}{(\alpha c_1)}} \quad (19)$$

For the Lyapunov function used in this study

$c_1 = \frac{1}{30}$; $R = \sqrt{30\frac{\beta}{\alpha}}$

Hence;

$$\Omega_R = \left\{X \in \mathbb{R}^3 : ||X|| \leq \sqrt{30\frac{\beta}{\alpha}}\right\}$$

III. RESULTS AND DISCUSSION.

Figure 1: Controlled Modal Displacement Response under Moving Vehicle Excitation

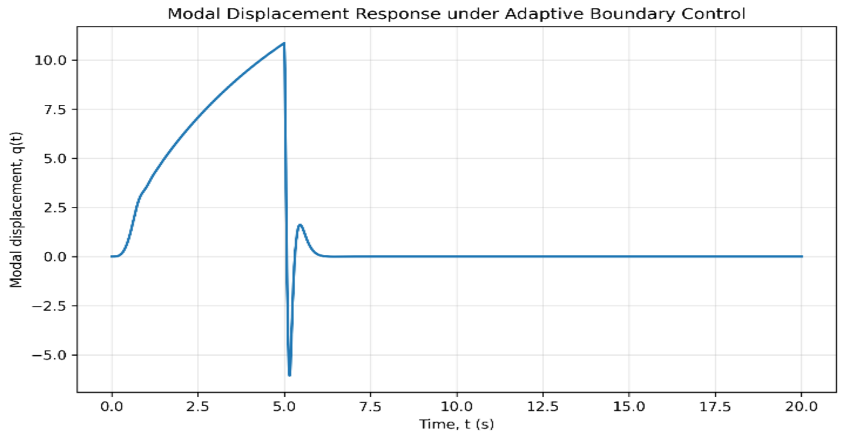

The controlled Modal Displacement Response under Moving Vehicle Excitation with different variation of parameters $m = 1.0$, $c = 0.8$, $k = 20.0$, $\Gamma = 15.0$, $L = 10.0$, $P = 10,000N$, $v = 2.0m/s$, $x_0 = q(0) = q(\dot{0}) = 0$, $\hat{k}(0) = 10.0$, $t_f = 20s$.

Figure 1 illustrates the temporal evolution of the fundamental modal displacement of the Euler–Bernoulli bridge under a moving vehicle load, uncertain boundary stiffness, and adaptive boundary control, with the response increasing to a peak of approximately at s before undergoing a transient reversal as the vehicle leaves the 10-m bridge. The subsequent rapid decay of the oscillations toward equilibrium demonstrates the dissipative effect of the adaptive controller in suppressing residual vibrations, while the Lyapunov formulation accounts explicitly for the moving vehicle as a bounded disturbance whose influence diminishes after the vehicle exits the bridge.

Figure 2: Controlled Modal Velocity Response under Moving Vehicle Excitation

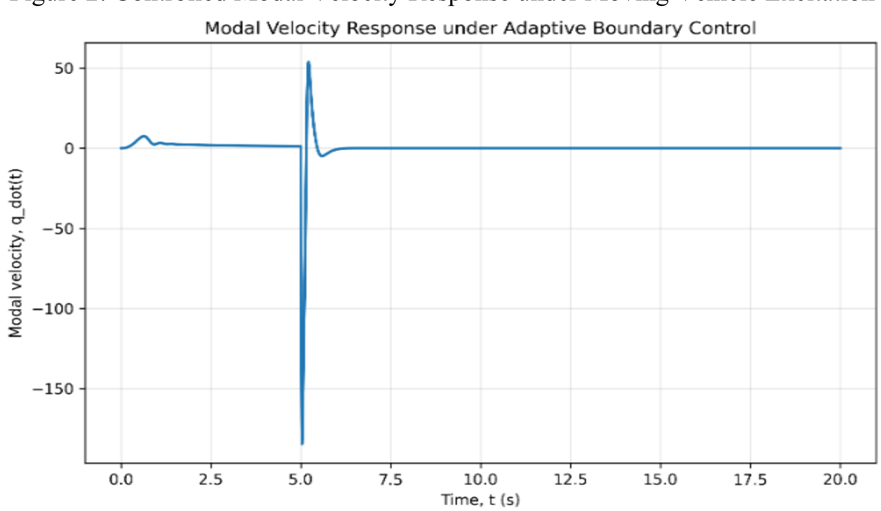

Controlled Modal Velocity Response under Moving Vehicle Excitation with different variation of parameters $m = 1.0$, $c = 0.8.$, $k = 20.0$, $\Gamma = 15.0$, $L = 10.0$, $P = 10,000N$, $v = 2.0m/s$, $x_0 = q(0) = q(\dot{0}) = 0$, $\hat{k}(0) = 10.0$, $t_f = 20s$.

Figure 2 illustrates the variation of the bridge's fundamental modal velocity during and after the passage of the moving vehicle. The velocity remains relatively small during the initial stage but exhibits a pronounced transient around, corresponding to the vehicle reaching the end of the bridge, after which the response quickly diminishes and approaches zero. This rapid attenuation demonstrates the effectiveness of the adaptive boundary controller in suppressing residual vibrations despite the uncertain boundary stiffness, while the transient response reflects the temporary influence of the moving vehicle as an external disturbance. The figure indicates that the controlled bridge system is able to restore the modal velocity to its equilibrium state following the disturbance, consistent with the stability characteristics established through the Lyapunov analysis.

Figure 3: Adaptive Boundary Stiffness Estimation under Moving Vehicle Loading.

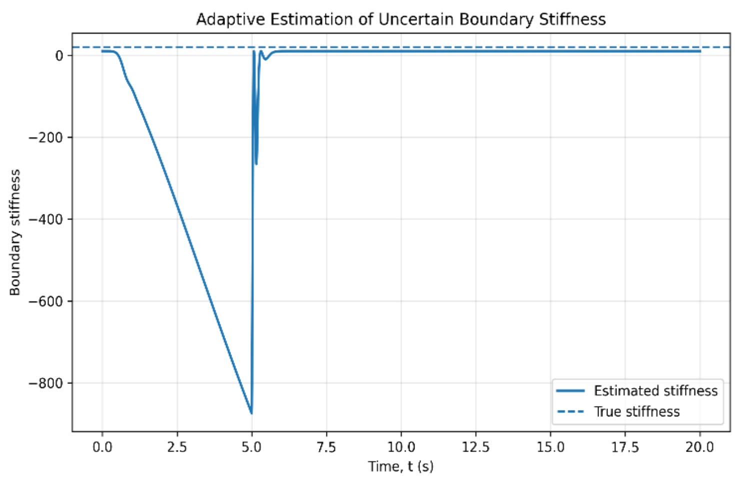

Adaptive Boundary Stiffness Estimation under Moving Vehicle Loading with different variation of parameters $m = 1.0$, $c = 0.8$, $k = 20.0$, $\Gamma = 15.0$, $L = 10.0$, $P = 10,000N$, $v = 2.0m/s$, $x_0 = q(0) = \dot{q(0)} = 0$, $\hat{k}(0) = 10.0$, $t_f = 20s$.

Figure 3 shows how the estimated boundary stiffness changes in response to the moving vehicle disturbance. As the vehicle travels across the bridge, the estimated stiffness decreases markedly, reaching its largest deviation around, when the vehicle leaves the 10-m bridge, after which the estimate rapidly recovers toward the nominal value. This transient behavior reflects the adaptive controller's response to the disturbance and uncertainty in the boundary stiffness, while the subsequent recovery indicates that the adaptive mechanism effectively compensates for these changes and helps restore the bridge system to its desired operating condition.

Figure 4: Boundary Stiffness Estimation Error under Moving Vehicle Excitation

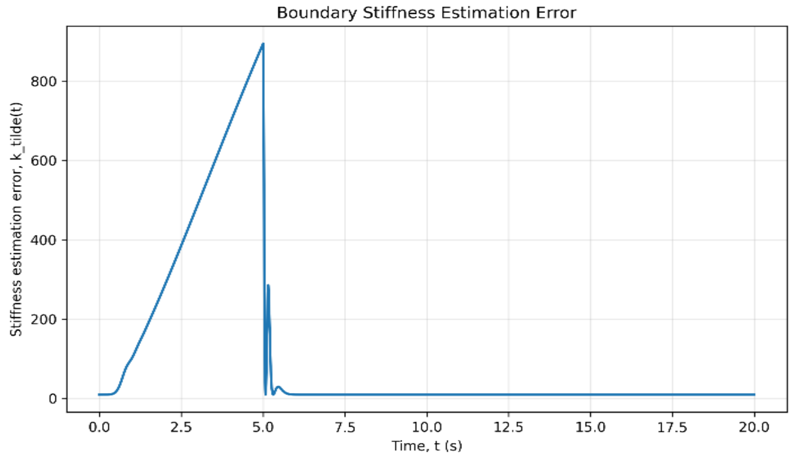

Boundary Stiffness Estimation Error under Moving Vehicle Excitation with different variation of parameters $m = 1.0$, $c = 0.8$, $k = 20.0$, $\Gamma = 15.0$, $L = 10.0$, $P = 10,000N$, $v = 2.0m/s$, $x_0 = q(0) = q(\dot{0}) = 0$, $\widehat{k}(0) = 10.0$, $t_f = 20s$.

Figure 5: Adaptive Control Input Response of the Euler–Bernoulli Bridge under Moving Vehicle Loading

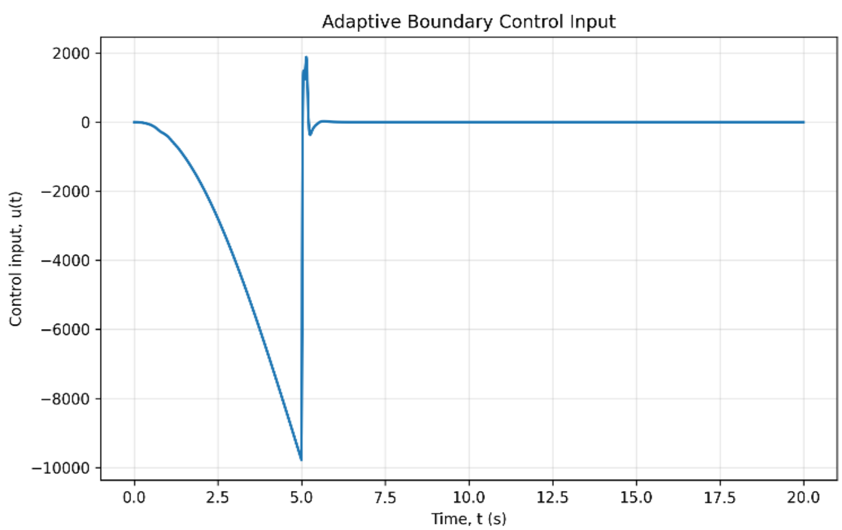

Adaptive Control Input Response of the Euler–Bernoulli Bridge under Moving Vehicle Loading with different variation of parameters $m = 1.0$, $c = 0.8$, $k = 20.0$, $\Gamma = 15.0$, $L = 10.0$, $P = 10,000N$, $v = 2.0m/s$, $x_0 = q(0) = q(\dot{0}) = 0$, $\widehat{k}(0) = 10.0$, $t_f = 20s$.

Figure 6: Time-Varying Moving-Vehicle Disturbance in the Adaptive Boundary-Controlled Bridge System.

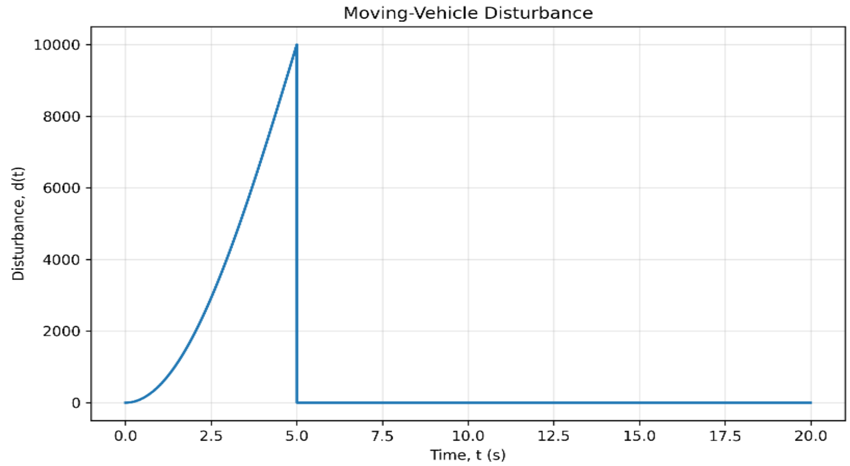

Time-Varying Moving-Vehicle Disturbance in the Adaptive Boundary-Controlled Bridge System with different variation of parameters $\boldsymbol{m = 1.0}$, $\boldsymbol{c = 0.8}$, $\boldsymbol{k = 20.0}$, $\boldsymbol{\Gamma = 15.0}$, $\boldsymbol{L = 10.0}$, $\boldsymbol{P = 10,000N}$, $\boldsymbol{v = 2.0m/s}$, $\boldsymbol{x_0 = q(0) = q(\dot{0}) = 0}$, $\boldsymbol{\widehat{k}(0) = 10.0}$, $\boldsymbol{t_f = 20s}$.

Figures 4–6 collectively illustrate the interplay among moving-load disturbance, adaptive parameter estimation, and control effort in the proposed boundary-control framework. As the vehicle traverses the bridge, the resulting time-varying disturbance induces a pronounced structural response, prompting the adaptive mechanism to adjust the estimated boundary stiffness while the controller generates the required corrective input to attenuate the induced vibration. Following the vehicle's departure from the bridge, the disturbance and control effort decrease rapidly, accompanied by a marked reduction in the stiffness-estimation error. These results demonstrate the capability of the proposed adaptive boundary-control strategy to accommodate uncertain boundary stiffness and effectively suppress transient structural vibrations induced by moving vehicle loads, thereby supporting the strength of the controlled Euler–Bernoulli bridge system.

Figure 7: Lyapunov Function Evolution under Adaptive Boundary Control and Moving Vehicle Excitation

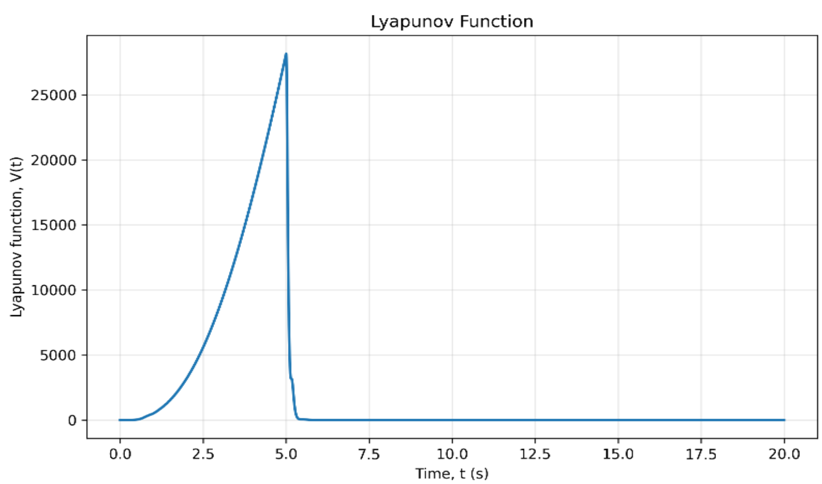

Boundary Control and Moving Vehicle Excitation with different variation of parameters $\boldsymbol{m = 1.0}$, $\boldsymbol{c = 0.8}$, $\boldsymbol{k = 20.0}$, $\boldsymbol{\Gamma = 15.0}$, $\boldsymbol{L = 10.0}$, $\boldsymbol{P = 10,000N}$, $\boldsymbol{v = 2.0m/s}$, $\boldsymbol{x_0 = q(0) = q(\dot{0}) = 0}$, $\boldsymbol{\widehat{k}(0) = 10.0}$, $\boldsymbol{t_f = 20s}$.

Figure 8: Strict Lyapunov Function Response of the Adaptive Boundary-Controlled Euler–Bernoulli Bridge under Moving Vehicle Excitation

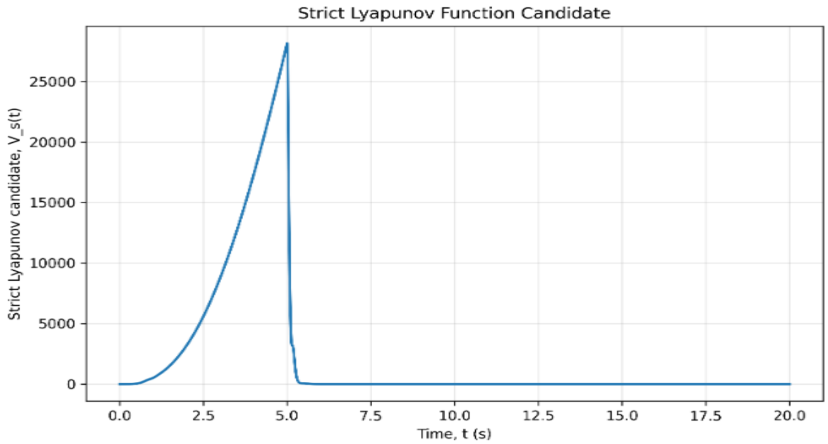

Strict Lyapunov Function Response of the Adaptive Boundary-Controlled Euler–Bernoulli Bridge under Moving Vehicle Excitation with different variation of parameters $\boldsymbol{m = 1.0}$, $\boldsymbol{c = 0.8}$, $\boldsymbol{k = 20.0}$, $\boldsymbol{\Gamma = 15.0}$, $\boldsymbol{L = 10.0}$, $\boldsymbol{P = 10{,}000N}$, $\boldsymbol{v = 2.0m/s}$, $\boldsymbol{x_0 = q(0) = q(\dot{0}) = 0}$, $\boldsymbol{\hat{k}(0) = 10.0}$, $\boldsymbol{t_f = 20s}$.

Figure 9: Moving Vehicle Position and Bridge-Exit Time

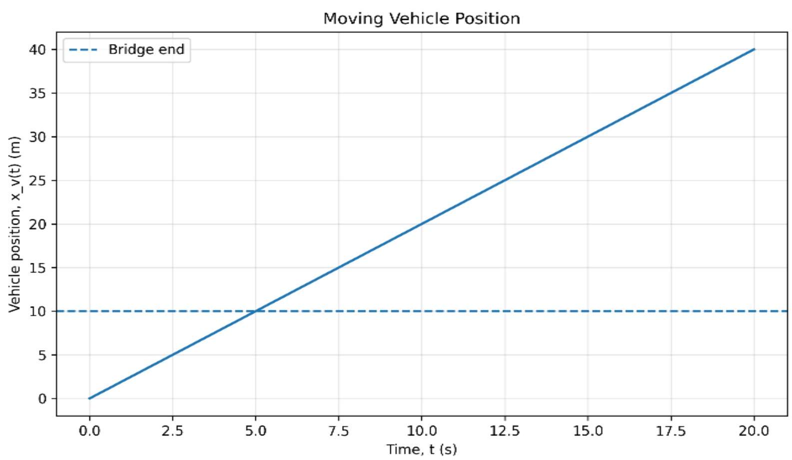

Moving Vehicle Position and Bridge-Exit Time with different variation of parameters $\boldsymbol{m = 1.0}$, $\boldsymbol{c = 0.8}$, $\boldsymbol{k = 20.0}$, $\boldsymbol{\Gamma = 15.0}$, $\boldsymbol{L = 10.0}$, $\boldsymbol{P = 10{,}000N}$, $\boldsymbol{v = 2.0m/s}$, $\boldsymbol{x_0 = q(0) = q(\dot{0}) = 0}$, $\boldsymbol{\hat{k}(0) = 10.0}$, $\boldsymbol{t_f = 20s}$.

Figures 7–9 collectively provide a clear picture of the stability and control performance of the Euler–Bernoulli bridge under moving vehicle excitation and uncertain boundary stiffness. Figure 7 shows that the Lyapunov function increases during vehicle passage and reaches its maximum around, reflecting the energy introduced into the bridge by the moving-load disturbance; following the vehicle's departure, the Lyapunov function decreases rapidly toward a small value, indicating effective dissipation of the residual vibrational energy by the adaptive controller. Similarly, Figure 8 shows a pronounced increase in the strict Lyapunov function during the loading period, followed by a rapid decline after, demonstrating that the controlled states and stiffness-estimation error are driven toward a bounded neighborhood of the desired equilibrium. Figure 9 provides the corresponding vehicle trajectory, with , where the vehicle travels at and reaches the bridge end at approximately ; this agrees with the major transient changes observed in Figures 7 and 8. The results indicate that the temporary increase in the Lyapunov measures is associated with the explicitly modeled moving-load disturbance rather than instability of the control system, while their subsequent decay demonstrates the ability of the adaptive boundary controller to dissipate the disturbance-induced energy and restore the bridge system toward its desired operating condition.

Figure 10: Transverse Deflection Profiles of the Adaptive Boundary-Controlled Euler–Bernoulli Bridge at Selected Times

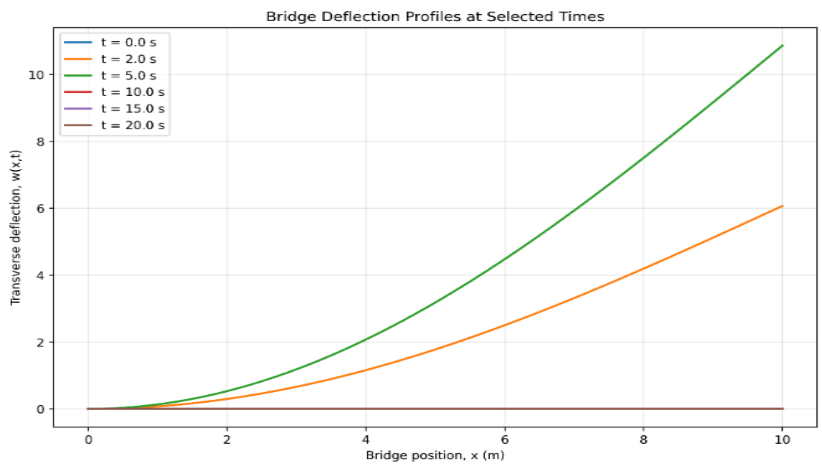

Transverse Deflection Profiles of the Adaptive Boundary-Controlled Euler–Bernoulli Bridge at Selected Times with different variation of parameters $\boldsymbol{m = 1.0}$, $\boldsymbol{c = 0.8}$, $\boldsymbol{k = 20.0}$, $\boldsymbol{\Gamma = 15.0}$, $\boldsymbol{L = 10.0}$, $\boldsymbol{P = 10,000N}$, $\boldsymbol{v = 2.0m/s}$, $\boldsymbol{x_0 = q(0) = q(\dot{0}) = 0}$, $\boldsymbol{\widehat{k}(0) = 10.0}$, $\boldsymbol{t_f = 20s}$.

Figure 11: Maximum Absolute Transverse Deflection Profile of the Adaptive Boundary-Controlled Euler–Bernoulli Bridge under Moving Vehicle Loading

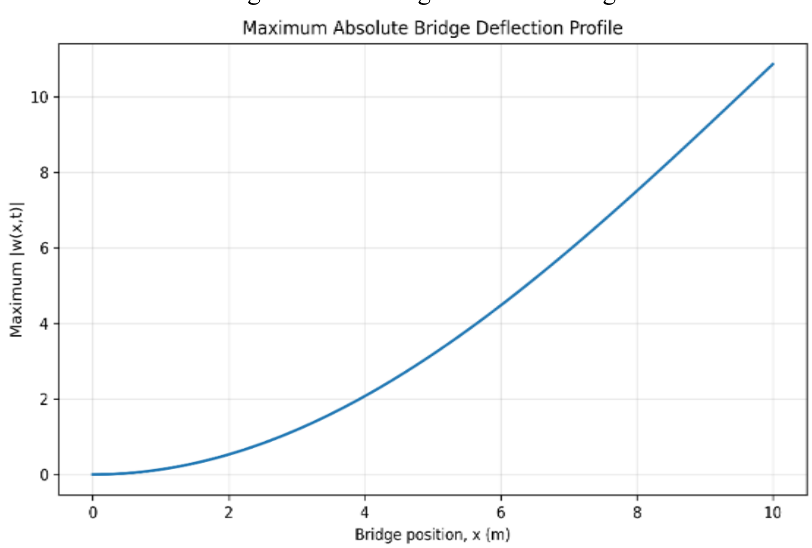

Maximum Absolute Transverse Deflection Profile of the Adaptive Boundary-Controlled Euler–Bernoulli Bridge under Moving Vehicle Loading with different variation of parameters $\boldsymbol{m = 1.0}$, $\boldsymbol{c = 0.8}$, $\boldsymbol{k = 20.0}$, $\boldsymbol{\Gamma = 15.0}$, $\boldsymbol{L = 10.0}$, $\boldsymbol{P = 10,000N}$, $\boldsymbol{v = 2.0m/s}$, $\boldsymbol{x_0 = q(0) = q(\dot{0}) = 0}$, $\boldsymbol{\widehat{k}(0) = 10.0}$, $\boldsymbol{t_f = 20s}$.

© AUG 2026 | IRE Journals | Volume 10 Issue 2 | ISSN: 2456-8880
DOI: https://doi.org/10.64388/IREV10I2-1722428

Figure 12: Analytical Lyapunov Derivative for Stability Assessment of the Adaptive Boundary-Controlled Euler–Bernoulli Bridge

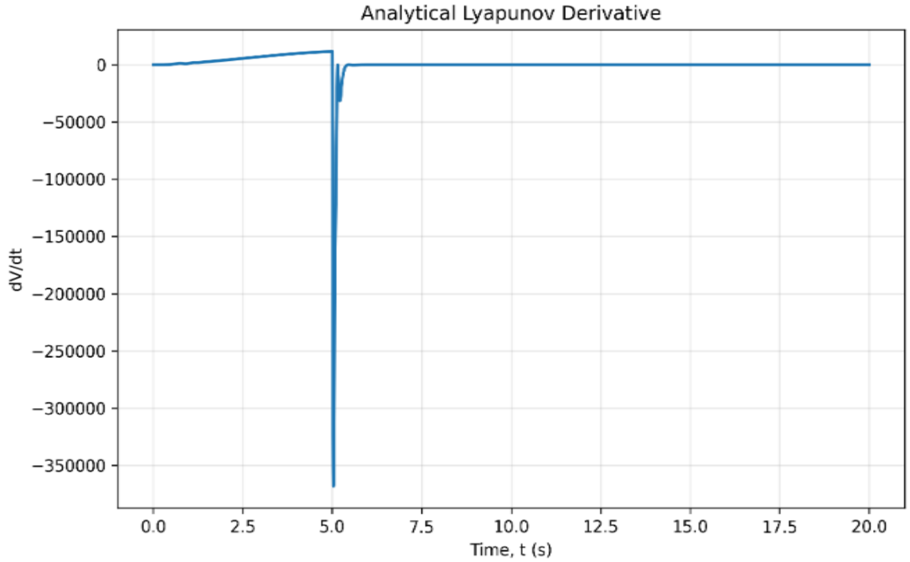

Analytical Lyapunov Derivative for Stability Assessment of the Adaptive Boundary-Controlled Euler–Bernoulli Bridge with different variation of parameters $\boldsymbol{m = 1.0}$, $\boldsymbol{c = 0.8}$, $\boldsymbol{k = 20.0}$, $\boldsymbol{\Gamma = 15.0}$, $\boldsymbol{L = 10.0}$, $\boldsymbol{P = 10,000N}$, $\boldsymbol{v = 2.0m/s}$, $\boldsymbol{x_0 = q(0) = q(\dot{0}) = 0}$, $\boldsymbol{\widehat{k}(0) = 10.0}$, $\boldsymbol{t_f = 20s}$.

Figures 9–12 collectively demonstrate the relationship between the moving vehicle, the resulting bridge deformation, and the stability of the proposed adaptive boundary-control system with uncertain boundary stiffness. The vehicle reaches the 10 m bridge exit at approximately, corresponding to the peak transient response, after which the bridge deflection and Lyapunov measures rapidly decrease as the disturbance disappears and the controller dissipates the remaining vibration. The results provide numerical support for the disturbance-inclusive Lyapunov analysis and indicate that the controlled bridge response remains bounded and progressively returns toward the desired equilibrium, consistent with the proposed UUB stability framework.

IV. CONCLUSION

This study developed an adaptive boundary-control framework for an Euler–Bernoulli overhead bridge subjected to moving vehicle loads in the presence of uncertain boundary stiffness. A Galerkin reduced-order model based on the fundamental mode was used to describe the bridge dynamics, while the adaptive control law was designed to compensate for stiffness uncertainty and reduce vehicle-induced vibrations. The moving vehicle was incorporated explicitly as a time-dependent bounded disturbance within the Lyapunov stability framework, enabling its influence on the controlled system to be systematically assessed.

The numerical results show that the vehicle produces a pronounced transient response, with the most significant structural effects occurring around, when the vehicle reaches the bridge exit. After the disturbance subsides, the modal displacement, velocity, control input, stiffness-estimation error, and Lyapunov measures decrease rapidly, demonstrating effective vibration suppression and bounded system behavior. Overall, the results indicate that the proposed adaptive boundary-control strategy can effectively manage uncertain boundary stiffness and mitigate transient moving-load vibrations, while the disturbance-inclusive Lyapunov analysis provides supporting evidence for the uniform ultimate boundedness (UUB) and improved dynamic stability of the controlled bridge system.

Acknowledgement.
The acknowledgement goes to the Department of Mathematics Rivers State University Port Harcourt, Nigeria.

REFERENCES.

[1] Abdelkarim, K., & Saedpanah, F. (2023). Stabilization of an axially moving Euler–Bernoulli beam by an adaptive boundary control. Journal of Dynamical and Control Systems, 29(3), 1–18. https://doi.org/10.1007/s10883-022-09632-y

[2] Cui, M., Yu, Y., & Yu, J. (2025). Event-triggered adaptive control of a rotating disk-beam-mass system with time-varying boundary constraint. Journal of the Franklin Institute, 362(18), 108243. https://doi.org/10.1016/j.jfranklin.2025.108243

[3] Dong, Y., Zhang, W., Shamsabadi, A., Shi, L., & Taciroglu, E. (2023). A vehicle–bridge interaction element: Implementation in ABAQUS and verification. Applied Sciences, 13(15), 8812. https://doi.org/10.3390/app13158812

[4] Gambarelli, S., Fararoni Platas, R. N., Shankar, A., Dakova, S., Böhm, M., Nitzlader, M., & Blandini, L. (2023). Failure behavior of an adaptive concrete beam with integrated fluidic actuators: Non-linear three-dimensional finite element analysis. Frontiers in Built Environment, 9, 1272785. https://doi.org/10.3389/fbuil.2023.1272785

[5] He, W., Zhang, S., Ge, S. S., & Liu, C. (2014). Adaptive boundary control for a class of inhomogeneous Timoshenko beam equations with constraints. IET Control Theory & Applications, 8(14), 1285–1292. https://doi.org/10.1049/iet-cta.2013.0601

[6] Krstić, M., & Smyshlyaev, A. (2008). Adaptive boundary control for unstable parabolic PDEs—Part I: Lyapunov design. IEEE Transactions on Automatic Control, 53(7), 1575–1591. https://doi.org/10.1109/TAC.2008.927798

[7] Ouyang, H. (2011). Moving-load dynamic problems: A tutorial (with a brief overview). Mechanical Systems and Signal Processing, 25(6), 2039–2060. https://doi.org/10.1016/j.ymssp.2010.12.010

[8] Pourzeynali, S., Zhu, X., Ghari Zadeh, A., Rashidi, M., & Samali, B. (2021). Comprehensive study of moving load identification on bridge structures using the explicit form of Newmark-β method: Numerical and experimental studies. Remote Sensing, 13(12), 2291. https://doi.org/10.3390/rs13122291

[9] Shi, Z., Mohammed, Y. M., Uddin, N., & Chen, G. (2024). A vehicle–bridge interaction model considering contact patch size and vehicle self-generated excitation: A theoretical study. Engineering Structures, 298, 117079. https://doi.org/10.1016/j.engstruct.2023.117079

[10] Smyshlyaev, A., & Krstić, M. (2007a). Adaptive boundary control for unstable parabolic PDEs—Part II: Estimation-based designs. Automatica, 43(9), 1543–1556. https://doi.org/10.1016/j.automatica.2007.02.014

[11] Smyshlyaev, A., & Krstić, M. (2007b). Adaptive boundary control for unstable parabolic PDEs—Part III: Output feedback examples with swapping identifiers. Automatica, 43(9), 1557–1564. https://doi.org/10.1016/j.automatica.2007.02.015

[12] Sun, L., Song, Y., Lv, M., Huang, X., & Wen, C. (2025). Event-triggered adaptive safe-oriented barrier Lyapunov function-based boundary control of flexible beam systems characterized by uncertain Euler–Bernoulli PDEs. Automatica, 182, 112555. https://doi.org/10.1016/j.automatica.2025.112555

[13] Wang, J., & Krstić, M. (2021). Adaptive event-triggered PDE control for load-moving cable systems. Automatica, 129, 109637. https://doi.org/10.1016/j.automatica.2021.109637

[14] Wang, Y., Wu, W., Lou, X., & Görges, D. (2025). Adaptive vibration control for stabilisation of the Euler–Bernoulli beam with an unknown payload. International Journal of Control, 98(7), 1573–1584. https://doi.org/10.1080/00207179.2024.2410854

[15] Xia, H., Xu, Y. L., & Chan, T. H. T. (2000). Dynamic interaction of long suspension bridges with running trains. Journal of Sound and Vibration, 237(2), 263–280. https://doi.org/10.1006/jsvi.2000.3027

[16] Yang, Y. B., & Lin, C. W. (2005). Vehicle–bridge interaction dynamics and potential applications. Journal of Sound and Vibration, 284(1–2), 205–226. https://doi.org/10.1016/j.jsv.2004.06.032

[17] You, T., et al. (2023). Distributed bending stiffness estimation of bridges using adaptive inverse unit load method. Engineering Structures, 297, 116981. https://doi.org/10.1016/j.engstruct.2023.116981